geographical analysis

Geographical Analysis (2015) **47,** 321–348

Investigating the Influence of Spatial and Temporal Granularities on Agent-Based Modeling

Eric Shook[1], Shaowen Wang[2]

[1]Department of Geography, Kent State University, Kent, OH, USA, [2]Department of Geography and Geographic Information Science, University of Illinois at Urbana—Champaign, Urbana, IL, USA

Epidemic agent-based models (ABMs) simulate individuals in artificial societies that are capable of movement, interaction, and transmitting disease among themselves. ABMs have been used to study the spread of disease at various spatial and temporal scales ranging from small communities to the world, over days, months, and years. The representations of space and time often vary between different epidemic ABMs and can be influenced by factors such as the size of a modeled population, computational requirements, population environments, and disease-related data. The influence that the representations of space and time have on epidemic ABMs is difficult to assess. Here we show that the finest representations of space and time—termed spatial and temporal granularities (STGs)—in a parsimonious ABM affect speed, intensity, and spatial spread of a synthetic disease. Specifically, we found disease spread faster and more intensely as spatial granularity is coarsened, whereas disease spread slower and less intensely as temporal granularity is coarsened in a parsimonious ABM. Our study is the first to use the same epidemic ABM to examine the influence of STGs. Our results demonstrate that STGs influence ABM dynamics including early disease burnout and that an interrelationship exists between the coarsening of STGs and the speed and intensity at which disease spreads. Our parsimonious ABM is extended based on a structured community model and we found STGs also influence ABM dynamics in a more realistic context that includes hierarchical movement. Broadly, our study serves as a basis for further inquiry toward the influence of space–time representations on more realistic models that include multiscale mobility, routine movements (e.g., commuting), and heterogeneous population distributions.

Introduction

Computational models are formulated to better understand complex spatiotemporal dynamics by comparing computer simulations to observations and theories. Although previous work in computational spatial modeling recognizes the importance of the embodiment of space and time (Bian 2004; Batty 2010; Batty et al. 2012; Manson, Sun, and Bonsal 2012), computational representations of space and time are often coarsened due to limitations in fine-scale

Correspondence: Eric Shook, Department of Geography, Kent State University, Kent, OH 44242, USA
e-mail: eshook@kent.edu

Submitted: November 17, 2013. Revised version accepted: March 17, 2015.

doi: 10.1111/gean.12080

understanding, data, and computational capabilities (Riley 2007; Ajelli et al. 2010; Hagen-Zanker and Jin 2012). This research investigates how the finest representations of space and time, termed spatial and temporal granularities (STGs), shape model processes—capturing movements and interactions of agents and environments—that operate within the constraints of such representations. Motivated by previous studies comparing epidemic models (Kaplan and Wein 2003; Ajelli and Merler 2008; Xu and Sui 2009; Ajelli et al. 2010), we formulate a novel modeling approach that makes disease models capable of adjusting to different STGs. We apply this approach to two disease models, providing a new spatial and temporal lens to critically examine epidemic models.

Disease spread is a complex, multi-scale process dispersing from an individual to a community, city, and country over days, weeks, and months. As a result, disease spread can be studied from a variety of spatial and temporal perspectives ranging from spatially and temporally fine grained to coarse grained (Fig. 1). Disease maps have long been used to understand disease spread (Snow 1855; Beyer, Tiwari, and Rushton 2012). Spatial analyses have been applied to studies of disease spread including for disease detection (Kulldorff and Nagarwalla 1995; Emch et al. 2012). Multiple studies have conceptualized epidemic disease spread as a wave moving through space and time to investigate spatial and temporal characteristics of disease spread based on historical diseases (Cliff and Haggett 2006; Cliff, Haggett, and Smallman-Raynor 2008). Disease models, including dynamic, cellular-automata, and agent-based ones, rely on simplifying assumptions to simulate disease spread in a computational model using desktop or high-performance computing (Hethcote 2000; Parker and Epstein 2011; Bian 2013).

Researchers and policy makers increasingly rely on epidemic agent-based model (ABM) simulations where individual agents move and interact passing disease among themselves to understand how communicable diseases such as influenza and smallpox may spread throughout

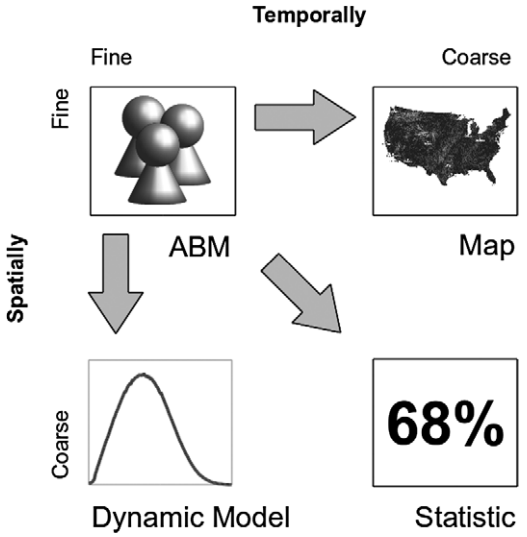

Figure 1. This figure illustrates a spectrum of spatial and temporal granularities situating fine-grained agent-based models (ABMs) with dynamic models that often have very coarse or no spatial representations, disease maps that often have coarse or no temporal representations, and disease statistics that capture a single spatially and temporally coarsened snapshot of disease. Different ABMs may lie at different points along this spatiotemporal spectrum.

a population (Ferguson et al. 2003; Epstein 2009). Comparing the results of these models that often differ in assumptions and STGs (Bobashev et al. 2007; Halloran et al. 2008; Ajelli et al. 2010) may lead to opposing interpretations (Kaplan and Wein 2003). Therefore, the influence of STGs on modeling results needs to be better understood in the context of epidemic modeling.

Our study systematically examines how variations of space–time representations affect the dynamics of two epidemic ABMs that are capable of adjusting to different STGs using a novel modeling approach as a first step toward developing techniques to deal with variations of space–time representations. Methodologically, our study is similar to the work on network-based epidemic models (Keeling 1999; Keeling and Eames 2005; Shirley and Rushton 2005; Xu and Sui 2009; Keeling et al. 2010) that seek to understand how alterations in network connections between agents influence the spread of disease. In both cases, synthetic models were manipulated to understand how changes in disease-spreading mechanisms (i.e., network connections or STGs) influence the spread of disease. Although spatial and temporal representations in ABMs have received significant attention (e.g., see excellent discussions in Parker et al. 2003; Batty 2012; Stanilov 2012; Bian 2013), the focus of discussion is often *the* scale(s), level(s) of detail, or granularity(ies) in an ABM. For example, O'Sullivan et al. (2012) introduce the spatial and temporal grain of a model representation to discuss differences in spatial ABMs such as comparing pedestrian models to land-use change models that operate at different grains ranging from seconds to years and meters to individual land parcels, respectively. Instead of focusing on a single granularity (or grain), we design an ABM that is capable of adjusting to different STGs, thus enabling our investigation into the influence of STGs on simulated disease spread while improving spatial and temporal understanding of modeling disease dynamics.

Space, time, and processes in epidemic models

A grand challenge for epidemic models is to accurately simulate disease spread in the absence of exact and complete data, including, for example, the locations of individuals and their homes or workplaces. Modelers face data limitations for both population and disease data, which are often coarsened due to concerns such as privacy (Maantay and McLafferty 2011). Data used to assign persons to workplaces or schools are also often aggregated or largely unavailable (Wheaton et al. 2009). Further, data are often lacking to understand where people may come into contact outside the home or workplace, termed unstructured contacts (Ajelli and Merler 2008). To compensate for limitations in data, epidemic models often rely on simplifying assumptions or abstractions, which may influence simulated disease dynamics including the locations of simulated individuals or with whom they contact.

Interactions among agents form contact or mixing patterns that are central to understanding how a disease spreads through populations (Koopman 2004). Mixing patterns include homogeneous (i.e., perfectly mixed) or heterogeneous, and are influenced by simplifying assumptions and model parameters (Mishra, Fisman, and Boily 2011), which often differ among ABMs including how agents move around and how a disease spreads from agent to agent (Ferguson et al. 2006; Germann et al. 2006; Atti et al. 2008). Changing spatial patterns of contact or mixing among agents is shown to influence simulated disease spread (Ajelli and Merler 2008; Ajelli et al. 2010). Although it is known that human mobility (Balcan et al. 2009; Brockmann 2009), agent-to-agent contacts (Bian 2004; Rahmandad and Sterman 2010), and duration of such contacts (Smieszek 2009) play an important role in agent-based modeling of disease spread, much less is

known about how variations of the representations of space and time determine when and where agents come into contact or the duration of agent contacts. This knowledge gap is considerable when compared with the field of spatial statistics that have well-developed approaches and methodologies for detecting and dealing with spatial biases or properties such as spatial dependence (Anselin and Rey 1991; Anselin 1995; Griffith 2006; Gumprecht, Müller, and Rodríguez-Díaz 2009; Haining, Kerry, and Oliver 2010). Arguably spatial and temporal dependence at the individual level is best understood in an ABM, because every agent interaction is defined in the computer code of a model. However, applying individual-level understanding to hundreds of simulations each consisting of thousands of individuals is a significant challenge. Although ABMs may benefit from new methodologies to deal with spatial biases and properties such as spatial or temporal dependence, a solid first step may be to shift the focus from designing ABMs for a single space–time representation to multiple space–time representations and to build an understanding of their influence.

Disease transmission modeling methods often adopted in spatial models can be categorized into four common abstractions (Riley 2007). We recast these within an agent-based modeling context for consistency within our discussion.

(1) **Group**. Disease transmission among groups of agents can only occur if they share a connection. Transmission rates among groups can vary, but agents within a group share the same rate of infection.
(2) **Network** models disaggregate groups into a network of agents in which transmission can only occur between connected agents.
(3) **Patch**. Agents within a patch share the same rate of infection, but disease transmission to nearby patches may occur at different rates usually based on distance between patches.
(4) **Distance** is calculated between susceptible and infectious agents to determine a rate of infection.

Embedded within each of the four abstractions lie distinctive assumptions about the representations of space for epidemic modeling that may influence disease spread. Patch and distance transmission methods *explicitly represent space* by relying on an agent's location. Whereas groups and networks *implicitly represent space* by relying on spatial characteristics such as agents' home, work, or school buildings to establish connections among groups or agents (Ferguson et al. 2006; Germann et al. 2006). These abstractions also specify different spatial granularities: *coarse to fine grained* (group and patch) and *very fine grained* (network and distance).

Time representation is critical to ABMs (Liu and Andersson 2004; Crooks and Castle 2012). Epidemic ABMs commonly use two types of time representation, namely continuous and discrete. Continuous time or event-based models operate on a temporally ordered sequence of events in which each event may change something in the model (e.g., an agent's location) or trigger a new event (Zeigler, Praehofer, and Kim 2000; Wainer and Mosterman 2011). Discrete–time models operate based on a global clock that ticks at fixed-time intervals (e.g., 6 or 12 h) and enforces agents in a model simulation to be updated simultaneously (Ferguson et al. 2006; Germann et al. 2006). More epidemic ABMs, particularly at a national or multinational scale, use discrete representations of time (Longini et al. 2004; Ferguson et al. 2006; Germann et al. 2006; Atti et al. 2008; Chao et al. 2010), which can be partially attributed to the challenges related to reformulating dynamics in terms of discrete events (Perumalla and Seal 2011).

A parsimonious epidemic ABM

Our study is novel in formulating a new modeling approach to investigate the influence of STGs on simulated disease spread. Our parsimonious epidemic ABM is capable of adjusting to different STGs through the use of a novel modeling approach such that a patch size (spatial granularity) of 10×10 m and time step duration (temporal granularity) of 1 h can be used in one simulation and a patch size of 500×500 m and time step duration of 8 h can be used in second simulation without modifying the ABM. This capability is distinctly different from other epidemic models and enables simulation results from the same ABM operating under different STGs to be compared to elucidate the influence of STGs rather than comparing results of different epidemic models that may be based on different assumptions or data (Halloran et al. 2008; Ajelli et al. 2010).

We sought parsimony in the design of our ABM to provide clear interpretation of results aimed toward improved understanding of the influence of STGs on ABM processes. Significant progress has been made in understanding the simulation of geographic processes (Albrecht 2005; Reitsma and Albrecht 2005), and we find similarities among prior approaches to coarsening STGs in the efforts of representing spatial–temporal dynamics in data models (Peuquet 1994; Yuan 2001; Goodchild and Glennon 2008). For example, Hornsby and Egenhofer (2002) examine how coarsening the granularity of time affects geospatial lifelines, which capture an individual's movement in a data model composed of time-stamped records of locations. Coarsening spatial granularities in an ABM aggregates finer grained spatial units into coarser (i.e., larger) spatial units, which is related to a well-known problem in the geography literature—the modifiable areal unit problem (MAUP) (Openshaw 1983). MAUP may occur if small spatial units (e.g., points or polygons) are aggregated into larger spatial units, whose configuration is modifiable, and where different configurations lead to different results (Openshaw 1983). Hornsby and Egenhofer (2002) examine how coarsening the granularity of time affects geospatial lifelines, which capture an individual's movement in a data model composed of time-stamped records of locations. However, the MAUP focuses on the problems related to spatial aggregation and does not explicitly address spatial processes (Goodchild 2004), and Hornsby and Egenhofer (2002) do not explicitly look at the influence of coarsening the granularity of time on the simulation of processes. Goodchild (2004) states that ABMs may be used to better understand processes by comparing a simulated world with the real world. This study uses simulations with the finest STGs as a proxy for the real world and compares these simulations with those of spatially and temporally coarsened simulations to improve understanding of the influence of STGs on ABM processes in the context of epidemic modeling.

The spatial landscape of our ABM consists of a grid of square patches whose edge length is controlled by a spatial granularity variable (*SG*). Several epidemic ABMs use gridded representations of space (Laskowski et al. 2011; Parker and Epstein 2011; Smieszek et al. 2011). Our ABM uses regularly sized and shaped patches to enable the systematic study of a range of spatial granularities from fine- to coarse-grained without complications related to aggregating irregularly shaped patches. The duration of discrete–time step in our ABM is controlled by a temporal granularity variable (*TG*). Our ABM adopts a discrete–time representation due to its widespread use in epidemic modeling (Longini et al. 2004; Ferguson et al. 2006; Germann et al. 2006; Atti et al. 2008; Chao et al. 2010).

Spatial and temporal extents (*SE* and *TE*, respectively) control the size of a spatial landscape and temporal duration of a simulation, and can be any multiple of *SG* and *TG*, respectively. The

Table 1 Primary Model Variables

Parameter	Name	Examples
SE	Spatial extent	16×16, $1{,}024 \times 1{,}024$
TE	Temporal extent	16, 64, 1,024
SG	Spatial granularity	1, 4, 16, 64, 256, 1,024
TG	Temporal granularity	1, 2, 8, 32, 128, 512
N	Number of agents	128, 1,024
S	Movement speed	1, 2
R	Infection radius	1, 2
P	Infection probability	20%, 50%, 70%
I	Infectious period	20, 64, 128
M	Spatiotemporal process model executions	10,000 or 1,000,000

other primary variables in our ABM include the number of agents (N), movement speed (S), infection radius (R), infection probability (P), infectious period (I), and number of simulations to execute in spatiotemporal process models (M), which are listed in Table 1. Movement speed controls how fast agents move across a spatial landscape. Infection radius controls how close two agents must be able to potentially transmit disease. Infection probability controls the chance of disease transmission when a susceptible agent is within an infectious agent's infection radius.

Our ABM adopts a commonly used susceptible, infectious, recovered epidemiological model to capture primary stages of a disease (Mishra, Fisman, and Boily 2011), which has been adopted or adapted by several epidemic modeling studies (Hethcote 2000; Xu and Sui 2009; Roche, Drake, and Rohani 2011). Most agents start each simulation being susceptible to disease. Upon disease transmission, agents become infectious and transmit disease to nearby susceptible agents for a fixed period, after which agents permanently recover from disease and are no longer susceptible.

Spatiotemporal process models

Processes in ABMs operate within the constraints of space–time representations, capturing spatiotemporal dynamics both implicitly and explicitly (Batty et al. 2012). Simplifying assumptions are often embedded in the processes designed to model dynamics to compensate for actions or behaviors that cannot be explicitly captured (Sattenspiel and Dietz 1995; Grimm et al. 2006; Riley 2007). For example, homogeneous mixing in epidemic models is commonly used (Ajelli et al. 2010; Mishra, Fisman, and Boily 2011) to grossly approximate individuals moving around and interacting at home, work, school, or a grocery store. Rather than explicitly simulating an infectious individual moving around in a school or workplace and infecting nearby students or coworkers, homogeneous mixing allows an infectious individual to attempt to infect every susceptible individual within a one mile radius. As STGs are coarsened, ABM processes may become increasingly challenged to explicitly capture dynamics such as movements and interactions within a simulation, instead relying on simplifying assumptions such as homogeneous mixing to implicitly capture dynamics. Within the context of spatially explicit epidemic ABMs, there is limited understanding of how commonly used simplifying assumptions (e.g., homogeneous mixing among agents) in ABM processes affect simulation results when STGs vary. This study formulates a novel approach—spatiotemporal process model—that helps to examine the influence of STGs on ABM processes.

A spatiotemporal process model contextualizes an ABM process within space and time allowing the influence of simplifying assumptions on simulation results to be examined as STGs are coarsened in ABMs. Defining a spatiotemporal process model enables modelers to specify how every variable, equation, and algorithm used in a process is situated in space and time. The modelers ask themselves, for example, how an infection probability variable that dictates the chance a susceptible agent is infected by an infectious agent should change if the duration of a discrete–time step (e.g., temporal granularity) is coarsened from 2 to 4 h. For example, modelers may question whether the infection probability variable should be doubled if the time step duration doubles to 4 h or perhaps be nominally increased by a certain amount given the fact that agents may part ways before the end of the fourth hour. Similarly, they ask how an infection probability variable should change if the spatial granularity of a lattice is coarsened from 10 km to 20 or 50. For example, modelers may question whether the infection probability variable should be decreased and by what amount when the spatial granularity is coarsened, because a larger patch size will likely result in an infectious agent interacting with greater numbers of susceptible agents. These questions help to reveal implicitly captured dynamics embedded in model assumptions such as an infection probability variable implicitly capturing agent movements and interactions as STGs are coarsened due to the inability of a model to explicitly represent the movements of an infectious and susceptible agent parting ways or coming into contact. The answers to these questions help to make these dynamics explicit, represented in a spatiotemporal process model. The undertaking of addressing these often-difficult questions deepens our knowledge of ABM processes by bringing to light their underpinning assumptions of space and time.

A spatiotemporal process model generates as output a set of probability matrices, each represented as a two-dimensional array P. Each cell in P represents the probability of a process occurring in a spatiotemporal region that surrounds the relative location of an individual agent, and whose size corresponds to a STG of a simulation (e.g., the size of a patch and duration of a time step). A probability matrix, for example, may be used by an ABM to define probabilities for an agent that is walking to remain in the same patch or move to a nearby patch each time step. Although spatiotemporal process models are not limited to probabilistic processes or two spatial dimensions, we use them as examples in this article. Each spatiotemporal process model may simulate a spatially and temporally explicit process such as agent–agent interactions, agent–environment interactions, or agent movements thousands of times in order to derive probabilities of process occurrence in a spatiotemporal region. Multiple probability matrices may be constructed for complex processes such as capturing differing probabilities of interaction among agents in different age categories (Germann et al. 2006).

Spatiotemporal process models do not eliminate simplifying assumptions or deal with properties such as spatial and temporal dependence; rather they provide a mechanism to examine how those assumptions and properties influence simulation results as STGs are coarsened in ABMs providing a first step toward developing methodologies to overcome them. In much the same way as spatial analysts appreciate the impact of spatial scales due to issues such as the MAUP (Wong 2009) and spatial dependence (Gumprecht, Müller, and Rodríguez-Díaz 2009; Haining, Kerry, and Oliver 2010), agent-based modelers appreciate the impact of spatial and temporal scales on their models (Bian 2004; Batty et al. 2012; Manson, Sun, and Bonsal 2012). However, as previously stated, due to limitations in fine-scale understanding, data, and computational capabilities ABMs often coarsen STGs (Riley 2007; Ajelli et al. 2010; Hagen-Zanker and

Jin 2012) and as a result often employ simplifying assumptions in a model based on a single spatial and temporal scale. By contextualizing ABM processes in spatiotemporal process models, ABMs become capable of adjusting to different STGs using constructed probability matrices. Different STGs correspond to different-sized spatiotemporal regions, which may change the size of probability matrices (e.g., number of regions) or the probabilities associated with particular regions. For example, the probabilities of an infectious agent transmitting disease to a susceptible agent residing in the same patch will likely be higher if the patch size is small, because the two agents will tend to be closer to each other providing more opportunities to transmit disease. If the patch size is very large, the agents will tend to be farther away reducing the chance of disease transmission. In other words, if a contagious person sits next to someone in a large stadium it is fair to say that the person sitting next to the contagious person has a higher chance of being infected due to spatial proximity compared with another person who is randomly seated anywhere in the stadium. To help illustrate how spatiotemporal process models can be used to examine the influence of STGs on model processes, we provide two concrete examples in the following sections.

Agent movement

Our ABM uses spatiotemporal process models to address a challenging question in modeling random agent movement in patch-based spatial representations: when should an agent move from one patch onto another? Previous approaches, including island, meta-population, and stepping-stone models, control movement largely through user-defined parameters, commuting, or travel data (Kareiva, Mullen, and Southwood 1990; Balcan et al. 2010; Keeling et al. 2010; Balcan and Vespignani 2012). In the absence of such data, particularly at spatial scales of a neighborhood or building complex, new approaches are needed for systematically determining agent movement across patches.

Our ABM assumes agents move around a spatial landscape by changing their direction randomly each step, commonly referred to as a random walk (Pearson 1905). Random walk, due to its jarring random changes in direction, distorts pedestrian movement at the finest spatial and temporal scales (Batty 2003). However, epidemic ABMs are often designed for coarser spatial and temporal scales, and random walk has been shown to capture human movement patterns at national scales (Brockmann, Hufnagel, and Geisel 2006) as well as on street networks (Jiang, Yin, and Zhao 2009). We adopt random walk as a mechanism for agents to move, similar to other epidemic models' adoption of random movement for agents (Epstein et al. 2008; Keeling et al. 2010).

We use a spatiotemporal process model, hereafter referred to as a movement model, to construct a probability matrix, hereafter referred to as a *movement_matrix*, that defines the probabilities for a randomly walking agent to remain in the same patch or move to a nearby patch each time step in our ABM. The spatially and temporally explicit movement model simulates a random walk process thousands of times to represent fine-grained agent movements that are used to construct a *movement_matrix*. Initially in the movement model, an agent is randomly assigned to a point-based location within an area the same size of a patch (e.g., spatial granularity) in an ABM simulation. The agent takes a number of steps in a random walk, proportional to the temporal granularity of a simulation. The random walk process is repeated numerous times, and each time the final location of the agent is recorded. Then, based on the final locations of each random walk and the STG of an ABM simulation, the movement model calculates the probabilities that agents remain within a same patch or move to a nearby patch. Probabilities derived from

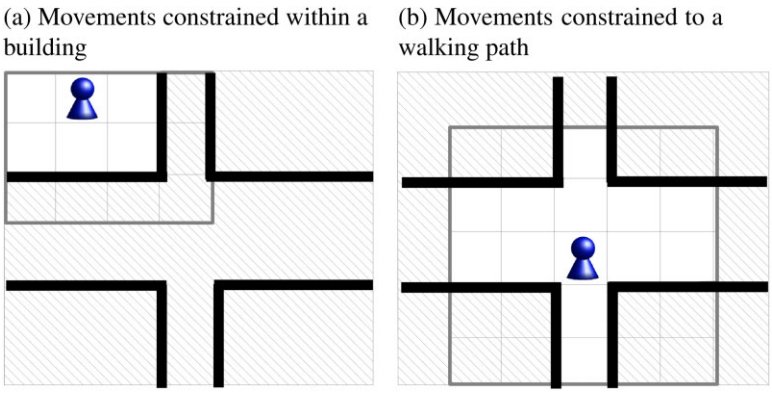

Figure 2. (a,b) This figure illustrates how agent movement using a 5×5 movement probability matrix may be constrained based on environmental barriers such as walls or walking path boundaries (thick black lines). If an agent attempts to walk to an area beyond a barrier (hatched gray lines), the movement process is restarted until a valid location is selected (illustrated as white patches in each figure). Notice in these figures that the same environmental barrier can be used in different contexts to restrict movement within a building and outside a building.

these simulations are used to construct a *movement_matrix*, which is used by our ABM to probabilistically move agents during a spatially and temporally coarsened simulation.

Movement matrices can be used by ABMs to facilitate probabilistic agent movement. In the simplest case, agents may be free to move to any location in a landscape, but in more complex cases environment barriers such as walls or water bodies may restrict agent movement. In these cases the movement process can be retried every time an agent attempts to move past a barrier such as a wall until a valid location is found (Fig. 2a). A similar process could be applied to walking paths, which could constrain agent movements to remain on patches associated with a walking path (Fig. 2b). If an environment barrier does not align with a patch edge, then traditional rasterization techniques can be used to determine whether a patch is inside or outside an environment barrier.

Agent infection

Agent infection in epidemic ABMs is a complex process involving multiple real-world dynamics (Ferguson et al. 2006; Germann et al. 2006; Atti et al. 2008). In temporally coarse ABMs, infection processes often implicitly capture agent movement through parameters, equations, and probabilities, because the duration of a time step (e.g., 6 or 8 h) is too long to explicitly capture finer grained movements (Ferguson et al. 2006; Germann et al. 2006). In spatially coarse ABMs, infection processes often capture disease transmission implicitly by assuming homogeneous mixing among agents within coarsened spatial landscapes (Mishra, Fisman, and Boily 2011). As STGs are refined, ABMs explicitly capture agent movement, and agent infection begins to match our understanding of disease transmission (Laskowski et al. 2011).

We use a spatiotemporal process model, hereafter referred to as an infection model, to construct a probability matrix, hereafter referred to as an *infection_matrix*, that facilitates agent infection in our ABM. The infection model is used to determine the probabilities of infection for susceptible agents in an ABM simulation based on whether they share the same patch or a nearby

patch with one or more infectious agents. Similar to the movement model, the infection model randomly places agents within areas the same size as a patch, and uses a random walk process to represent fine-grained agent movements. Unlike the movement model, the infection model simulates two agents, in which an infectious agent attempts to infect a susceptible agent if it is within an infection radius, *R*, after each step in a random walk. The movement model simulates numerous pairs of agents to calculate the probabilities of infection if a susceptible agent is located within a same patch or nearby patch of an infectious agent in our patch-based ABM. Using a concrete example, we illustrate the design and application of our ABM, movement model, and infection model in the following section.

Illustration of models

We illustrate a straightforward example of our ABM consisting of five agents walking around a spatial landscape of size 8×8. We compare two cases: a spatial landscape is represented as a 4×4 grid of smaller patches in one case and a 2×2 grid of larger patches in the second case (i.e., $SG = 2$ or $SG = 4$, respectively). The agents in our illustration—labeled A, B, C, D, E—are each randomly assigned to a patch and randomly walks around the landscape, transmitting disease with 90% probability to susceptible agents within a distance of 0.8 while infectious. One randomly selected agent is infected at the beginning of a simulation. The duration of a time step is 2 (e.g., temporal granularity) and walking speed for all agents is 0.3. We detail a (*a*) movement model; (*b*) infection model; and (*c*) parsimonious epidemic ABM for the $SG = 2$ cases and then repeat the steps for the $SG = 4$ cases demonstrating our approach and providing two concrete scenarios to compare.

Before a simulation begins, our patch-based ABM uses a spatially and temporally explicit movement model that simulates a fine-grained random walk process (Fig. 3a) numerous times to derive probabilities of agent movement across patches based on the spatial granularity, temporal granularity, and movement speed. In the $SG = 2$ cases, the movement model calculates that agents remain in the same patch 77% of the time, move to an adjacent patch approximately 5% of the time or to a cornering patch 0.3% of the time based on one thousand random walks (Fig. 3b). The movement model constructs a probability matrix named *movement_matrix* based on these probabilities.

Similarly, our patch-based ABM uses a spatially and temporally explicit infection model that simulates two randomly walking agents—one infectious trying to infect the other that is susceptible (Fig. 4a)—numerous times to derive probabilities of infection for susceptible agents occupying patches nearby infectious agents (Fig. 4b). The infection model is repeatedly executed, each time initially locating a susceptible agent in a different nearby area corresponding to a patch in our ABM (Fig. 4c). In each infection model simulation, the two agents proceed to randomly walk, and after each step, the infectious agent attempts to infect the susceptible agent if it is near. In the $SG = 2$ cases, the infection model calculates that susceptible agents have a 51% probability to become infected if they share a patch with an infectious agent, approximately 6% if they are in an adjacent patch or 0.6% in a cornering patch to an infectious agent based on thousands of simulated agent pairs. The infection model constructs a probability matrix named *infection_matrix* based on these probabilities.

Following the construction of probability matrices, *movement_matrix* and *infection_matrix*, our parsimonious ABM begins executing a simulation. First, our ABM assigns each of the five agents to a randomly selected patch and infects a random agent (agent E in our example) (Fig. 5a). Next, the ABM executes a series of iterations (*TE*/*TG*) that (*a*) use the

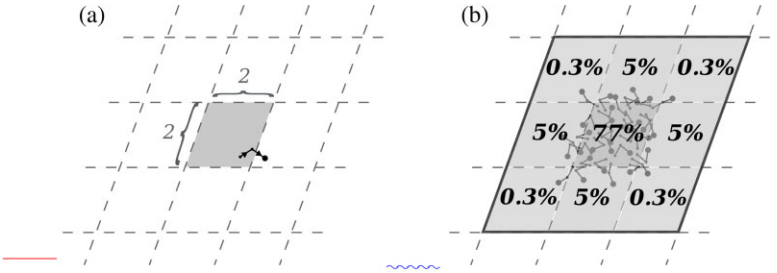

Figure 3. Illustration of a movement model that calculates probabilities of agents moving across patches based on the spatial and temporal granularities of an agent-based model (ABM) simulation using a random walk process. The parameter configurations in this illustration limit agent movements to adjacent and cornering patches, but certain parameter configurations may result in agents walking to non-adjacent patches (e.g., two, three, or more patches away) and thus the probability matrix will increase in size from 3×3 to 5×5 or 7×7, for example. (a) Randomly select an explicit point-based location for an agent within a spatial area the size of a patch (i.e., 2×2). Randomly walk the agent, moving it distance $S = 0.3$ in a random direction $TG = 2$ times (i.e., the duration of a time step in our ABM). The duration of a time step in our ABM determines the number of steps in a random walk. (b) Repeat 3a $M = 1{,}000$ times, counting the number of agents that moved to nearby areas or remained within the initial area to derive probabilities of agents moving to nearby patches or remaining within the same patch, which are used to construct a probability matrix named *movement_matrix* to be used by our ABM. Probabilities are truncated for brevity.

movement_matrix to probabilistically move each agent (Fig. 5b) and (*b*) use the *infection_matrix* to probabilistically infect susceptible agents near infectious agents (Fig. 5c). Notice, in Fig. 5c that agent E has 6% and 0.6% probability of infecting agents B and D, respectively, and that agents A and C cannot be infected, because they cannot be reached by agent E given the walking speed, temporal granularity, infection radius, and their locations. In the next time step, both agents E and B use the *infection_matrix* to try to infect nearby susceptible agents.

We repeated the aforementioned steps, while coarsening the spatial granularity to $SG = 4$ and show an example of agents as being randomly assigned to one of the four patches in Fig. 5d. The *movement_matrix* and *infection_matrix* for the $SG = 4$ cases are shown in Fig. 5e and 5f, respectively, for comparison. We draw the reader's attention to the exposure of all susceptible agents to infection from agent E due to a coarsened spatial granularity, as well as different infection probabilities for B and D and movement probabilities for all agents. Further, in the next time step agent C will attempt to infect the remaining susceptible agents in addition to agent E, raising the chance of infection for agents A, B, and D. The remainder of this article elucidates how coarsening STGs influence model processes and disease spread dynamics.

Experimental results

The goals of this study are to understand the influence of STGs on model processes and to build a foundation of spatial and temporal knowledge of epidemic simulations. Our goals are similar to those of network-based epidemic model studies that gain new insights into how disease spreads across networks of varying configurations, and whose results show that network configurations

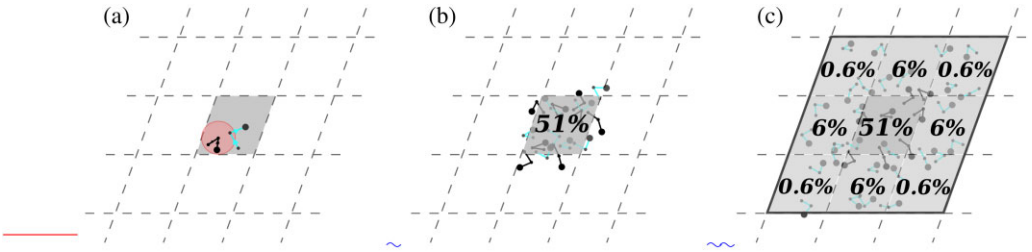

Figure 4. Illustration of an infection model that calculates probabilities of infection for susceptible agents occupying patches nearby infectious agents based on the spatial and temporal granularities of an agent-based model (ABM) simulation. Certain parameter configurations may result in calculating infection probabilities for larger numbers of patches (e.g., 5×5 or 7×7). (a) Randomly select explicit point-based locations for one susceptible (blue) and one infectious agent (black) within a spatial area the size of a patch (i.e., 2×2). Randomly walk each agent, moving them distance $S = 0.3$ in a random direction $TG = 2$ times. For each step, if the agents are within distance $R = 0.8$ (red area), then probabilistically transmit disease $P = 90\%$. Notice potential infection after first step (i.e., agents are within infectious radius R). (b) Repeat 4a M = 1,000 times, counting the number of infections between the pairs to derive infection probabilities for susceptible agents occupying the same patch as an infectious agent. (c) To calculate probabilities of infection for susceptible agents not sharing a patch with an infectious agent, initially locate the susceptible agent in a nearby area corresponding to an adjacent or cornering patch, for example, and repeat the process in panels (a) and (b). Execute the model for all nearby areas and calculate probabilities of infection for each area to construct a probability matrix named *infection_matrix* to be used by our ABM. Probabilities are truncated for brevity.

can significantly influence disease spread dynamics (Keeling 1999; Keeling and Eames 2005; Shirley and Rushton 2005; Xu and Sui 2009; Keeling et al. 2010). Our study assesses changes in speed, intensity, and spatial spread of a synthetic disease to investigate the influence of STGs on model processes in an ABM. Following the methodologies used in the network-based studies, we sought parsimony in the design of a synthetic model, rather than focusing on matching population distributions, disease characteristics, and movement patterns (see, e.g., Grassly and Fraser 2008 and Prieto et al. 2012). Conceptually, a simulation of our synthetic model may represent disease spread at various spatial or temporal scales ranging from a national, state, county, city, or building scale spanning years, months, days, or hours based on the parameters used.

We use the following baseline parameters for our study and conduct sensitivity analysis altering these baseline parameters to understand their influence. We construct a scenario for conceptual exploration consisting of 1,024 agents that may represent more than one individual on a landscape with spatial extent 128×128 km and temporal extent of 512 h (approximately 21 days). One randomly assigned agent is infected at the beginning of a simulation. Infectious agents infect susceptible agents within a radius of 5 km with 20% probability of infection for 16 h (i.e., infectious period). Agents randomly walk at a speed of 5 km/h, the average walking speed for humans. The results are averaged over 10,000 simulations for each parameter configuration. Due to the large number of simulations per parameter configuration, we re-use movement and infection matrices for 2,000 ABM simulations (M = 1,000,000), which has little influence on simulation results. We examine six spatial granularities with edge lengths equal to 1, 2, 4, 8, 16, and 32 km and four temporal granularities with time step durations equal to 15, 30, 60, and

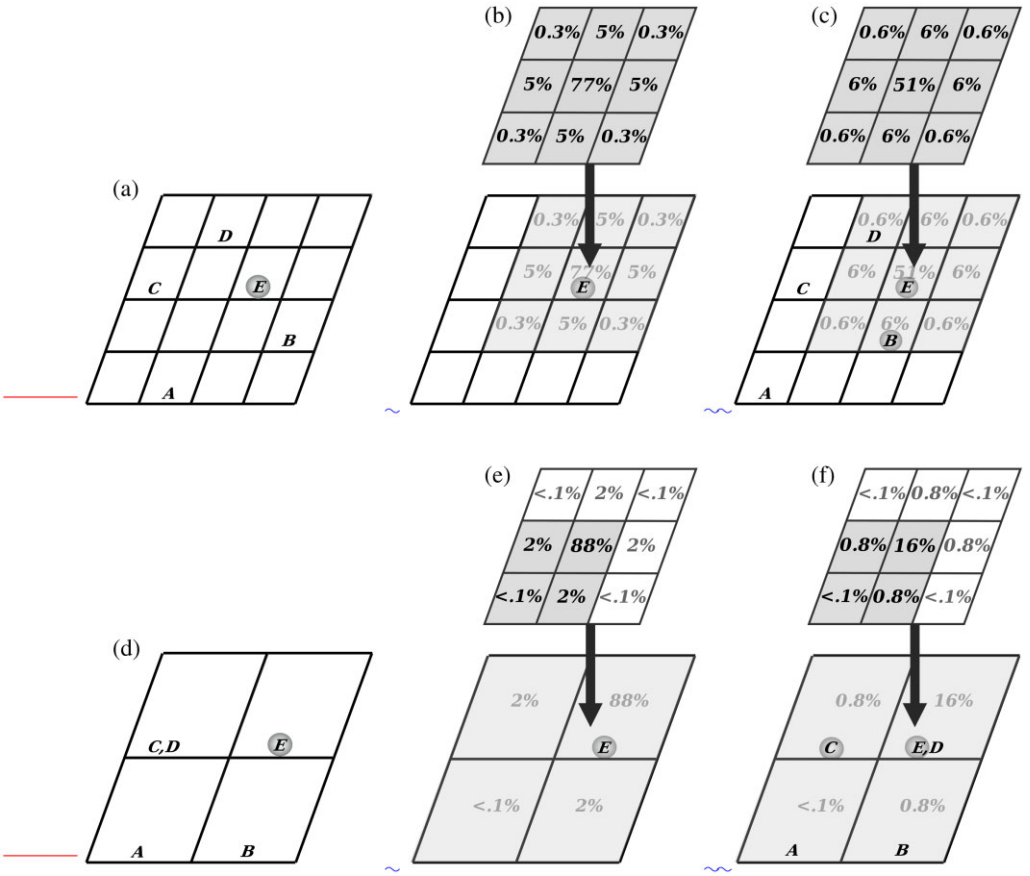

Figure 5. Illustration of the steps in our patch-based agent-based model comparing $SG = 2$ (a–c) and $SG = 4$ (d–f). Movement and infection probabilities for agent E are shown in the steps for comparison. (a) Randomly assign each agent (A–E) to a patch. Randomly infect one agent (agent E in our example). (b) Move each agent based on the probabilities defined in the *movement_matrix*. Movement probabilities to nearby patches for agent E are shown. (c) For each infectious agent, probabilistically infect nearby susceptible agents (e.g., B) based on *infection_matrix*. (d) Randomly assign each agent (A–E) to a patch. Note that patch size has changed from 2×2 to 4×4 reducing the number of patches from 16 to 4. (e) Probabilistically move each agent based on a *movement_matrix* constructed for a 4×4 patch size. If an agent attempts to walk beyond a landscape boundary, then retry random movement. (f) For each infectious agent, probabilistically infect nearby susceptible agents (e.g., C) based on *infection_matrix*, which is constructed by simulating the infection model with a 4×4 patch size.

120 min. The finest grained simulations with a spatial granularity of 1×1 km and temporal granularity of 15 m are used as a proxy for the real world, which are compared with spatially and temporally coarsened simulations.

A movement and an infection spatiotemporal process model construct movement and infection probability matrices, respectively, enabling our ABM to adjust to different STGs in our experiments. To construct a movement probability matrix, first an agent is randomly placed in an area the size of a patch ranging from 1×1 km to 32×32 km. The agent randomly walks for the

duration of a time step ranging from 15 to 120 min at a speed of 5 km/h. The final location of the agent is recorded and the process is repeated 1,000,000 times. The probabilities that an agent will remain on the same patch or move to nearby patches are calculated based on the final locations of the agents and are used to construct a movement probability matrix. The construction of the infection probability matrix is similar to the movement probability matrix. Through the use of spatiotemporal process models, the same spatial processes (e.g., movement and infection) based on the same parameters (e.g., walking speed, infection radius, and infection probability) are used for all simulations enabling the examination of the influence of STGs in our parsimonious epidemic ABM.

Speed and intensity of disease

Attack rate curves plot new infections across the duration of an epidemic, capturing disease spread over time. They are often characterized by their peaks, termed peak attack rate (PAR), and when the peak occurred, termed time of peak attack rate (TPAR) (Ferguson et al. 2006; Xu and Sui 2009; Ajelli et al. 2010). The PAR and TPAR help to quantify the intensity and speed of disease spread, describing the maximum number of individuals infected in a single period, at which point the disease has saturated the population, and how quickly the disease reaches saturation. The spatially and temporally finest grained simulations—a proxy for the real world in our study—result in a relatively low PAR infecting only 1.18% of the population at peak with a TPAR occurring at 102 h (approximately 4 days) on average. In general, we find that coarsening spatial granularity results in significantly higher PAR, infecting almost 8% of the population at peak, whereas coarsening temporal granularity results in comparatively lower increase in PAR infecting around 5% of the population at peak (Fig. 6). We also examine the percentage of agents that became infected during a simulation, termed cumulative attack rate (CAR), and find that coarsening spatial granularity in our simulations influences PAR, TPAR, and CAR more than coarsening temporal granularity overall (Fig. 7). However, space and time remain interwoven based on our simulation results, and generally, TPAR in spatially fine-grained simulations occurs earlier if temporal granularity is more coarse, whereas TPAR in spatially coarse-grained simulations occurs earlier if temporal granularity is fine (Fig. 7b), which was also observed in other parameter combinations not included in the article. Interestingly, we found a non-linear relationship between PAR and TPAR when coarsening STGs (Fig. 8a) compared with a linear relationship found in reconfiguring links in small-world network-based epidemic simulations (Xu and Sui 2009). Further studies may help to elucidate these differences, potentially adding value to recent work in studying contact networks that seek to bridge spatial proximity and networks (Salathé and Jones 2010).

Understanding how coarsening STGs influence early disease spread (Ferguson et al. 2003) is important to understanding the chance that a disease becomes an epidemic or burns out, infecting a few individuals but not spreading to the larger population (Rahmandad and Sterman 2010). In general, we find that coarsening spatial granularity reduces the chance of early disease burnout in simulations in some cases to 2.5% whereas coarsening temporal granularity increases the chance of early disease burnout in some cases to more than 6% (Fig. 9a). Coarsening spatial granularity also speeds the initial spread of disease to 1% of the population from an average simulated time of almost 13 h compared with almost 18 h (Fig. 9b). We modify the measure for early disease burnout in Rahmandad and Sterman (2010), from failing to infect 10% of the population or less to failing to infect 1% of the population or less, and remove the results from these simulations from further analyses. We use the time to infect 1% of the population as a

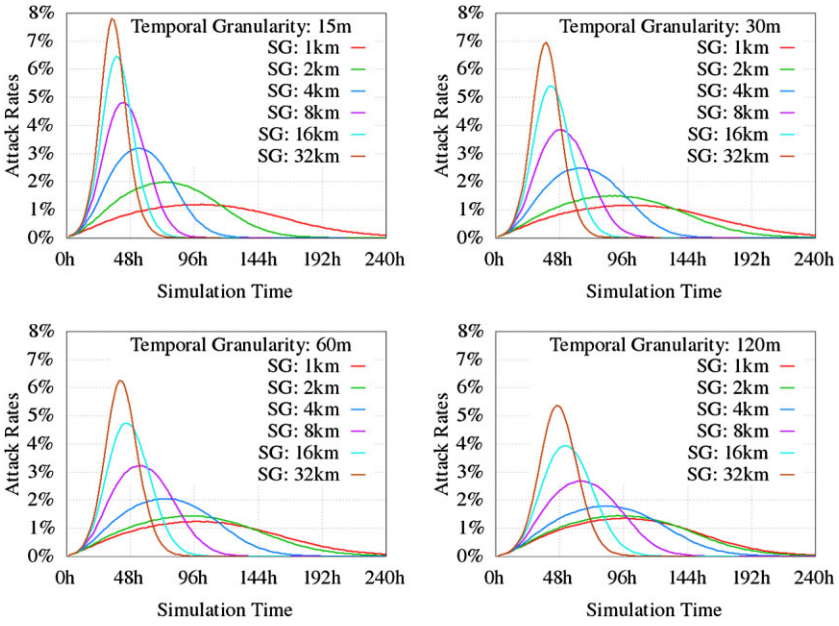

Figure 6. The four attack rate curves plot new infections every 2 h as a percentage of total population for different spatial and temporal granularity configurations. The real-world proxy representing a spatial granularity (SG) of 1 km and temporal granularity (TG) of 15 min is located in the upper left plot.

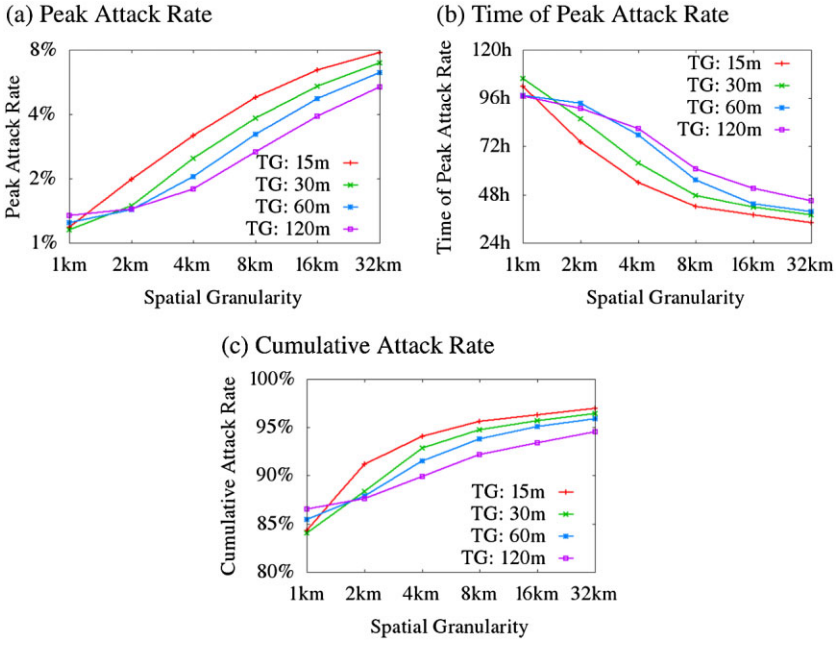

Figure 7. (a) Peak attack rate (PAR), (b) time of PAR, and (c) cumulative attack rate as spatial granularity is coarsened from 1 to 32 km and temporal granularity is coarsened from 15 min to 2 h.

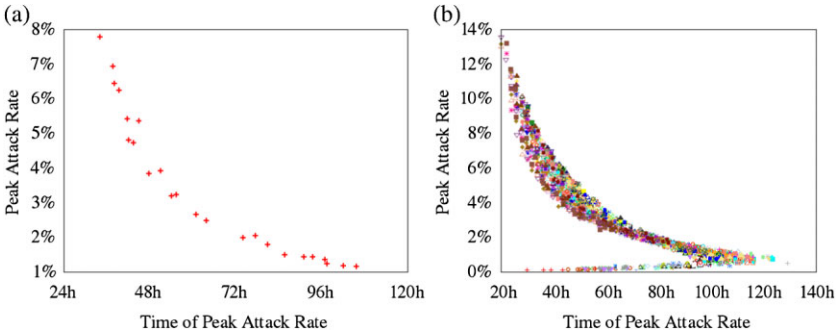

Figure 8. The two plots illustrate the relationship between average peak attack rate (PAR) and time of PAR for all configurations of spatial and temporal granularities (STGs) tested (a) and a sensitivity analysis (b). (a) Each sample represents one STG configuration as spatial granularity is coarsened from 1 to 32 km and temporal granularity is coarsened from 15 min to 2 h. (b) Each sample represents one parameter and STG configuration. Each parameter configuration shares the same symbol to illustrate the influence as STGs are coarsened.

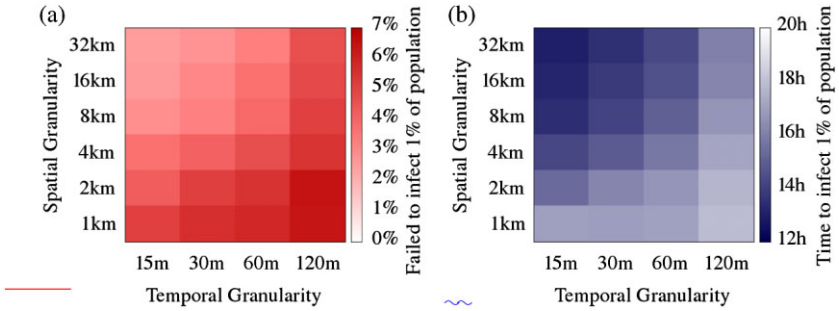

Figure 9. The two plots illustrate the influence of spatial and temporal granularities (STGs) on early disease spread dynamics. (a) Illustrates the percentage of simulations in which disease failed to infect at least 1% of a population. These simulations were removed from further analyses. (b) Average simulation time to infect 1% of a population.

measure of initial speed of disease spread similar as used in Danon, House, and Keeling (2009). We found initial spread to 10% of the population to have similar trends as 1%. Our results are consistent with network-based modeling results (Keeling 1999) in showing that increased spatial structure, in our case finer spatial granularities, and their case increased numbers of shared neighbors, play an important role in determining the chance of success or failure of an epidemic early in a simulation of disease spread.

We conducted sensitivity analysis (Table 2) and plot the relationship between PAR and TPAR for all parameter combinations (Fig. 8b). Sensitivity analysis shows a non-linear relationship between PAR and TPAR. In general, a lower PAR will peak at a later simulation time, except when PAR is below a certain threshold (e.g., approximately 1% of the population) in which case it occurs earlier. The peak is so small below this threshold that it becomes increasingly more likely to peak earlier in the simulation. When comparing maximum PAR of all STG combinations against our baseline simulations (7.7%), we find that increasing walking speed (S) from 5 to 6 km/h increases maximum PAR to 7.9%, infection radius (R) from 5 to 6 km results in increases

Table 2 Sensitivity Analysis Parameters

Parameter	Start value	End value	Increment
Infection probability (P)	15%	25%	5%
Walking speed (S)	4 km/h	6 km/h	0.5 km/h
Infection radius (R)	4 km	6 km	0.5 km

We executed 5,000 simulations for each parameter configuration.

to 11%, and infection probability (*P*) from 20 to 25% increases maximum PAR to 9.8%. We reduced each of the three variables (*S*, *R*, and *P*) to 4 km/h, 4 km, and 15%, which resulted in maximum PAR of 7.0, 4.1, and 5.4%, respectively.

Although the influence of STGs on the speed and intensity of disease is stark, it is not a complete picture. Attack rate curves are commonly used to capture disease spread in epidemic model simulations, but only provide a temporal view of disease spread. To fully understand disease dynamics and the underlying causes of peaks and valleys in attack rate curves, we also investigate spatial characteristics of disease spread.

Spatial spread of disease

Disease spread unfolds in both time and space, and so we spatially contextualize our results using a swash-backwash model, which is designed to capture and analyze the leading and trailing edges of disease spread (Cliff and Haggett 2006). A swash-backwash model divides a spatial area (e.g., simulated landscape) into subareas. For each subarea, a swash-backwash model records the time of the first infection occurrence (leading edge of disease spread) and last infection occurrence (trailing edge). For each time period, the model subtracts the number of trailing edge subareas by leading edge subareas. Spatial spread of disease is visualized by plotting the difference in leading and trailing areas over time.

We apply a swash-backwash model to our simulation results, dividing the 128×128 km simulated landscape into 8×8 km sized subareas and plot the difference in leading and trailing areas (Fig. 10). At the beginning of a simulation, new infections increase leading edge areas (positive values) as disease spatially spreads. As agents recover from disease, there are fewer new infections and trailing edge areas (negative values) increase leading to an overall decline in spatial area until the disease dies out.

We use a swash-backwash model to understand why coarsening spatial granularity increases PAR and CAR (Fig. 7a and 7c, respectively). The swash-backwash model results show that coarsening spatial granularity generally leads to a higher peak in leading edge area (Fig. 10). Two factors contribute to higher peaks in leading edge area. First, coarsening spatial granularity influences the movement process by obscuring fine-grained precision of an agent's location and as a result, agents may move longer distances each time step. Acknowledging that agents may reside along an edge of a patch and thus each time step may move to an adjacent patch, the patch size can influence the distance an agent can travel each time step. If an agent travels across two adjacent patches, for example, the distance can be significantly different if the spatial granularity is 2×2 km compared with 32×32 km (i.e., 2 km compared with 64 km travelled, respectively). Second, coarsening spatial granularity influences the infection process by increasing the size of patch and nearby patches, thereby exposing more susceptible agents to potential infection by infectious agents. As the patch sizes increase from 1×1 km to 32×32 km, the number of agents

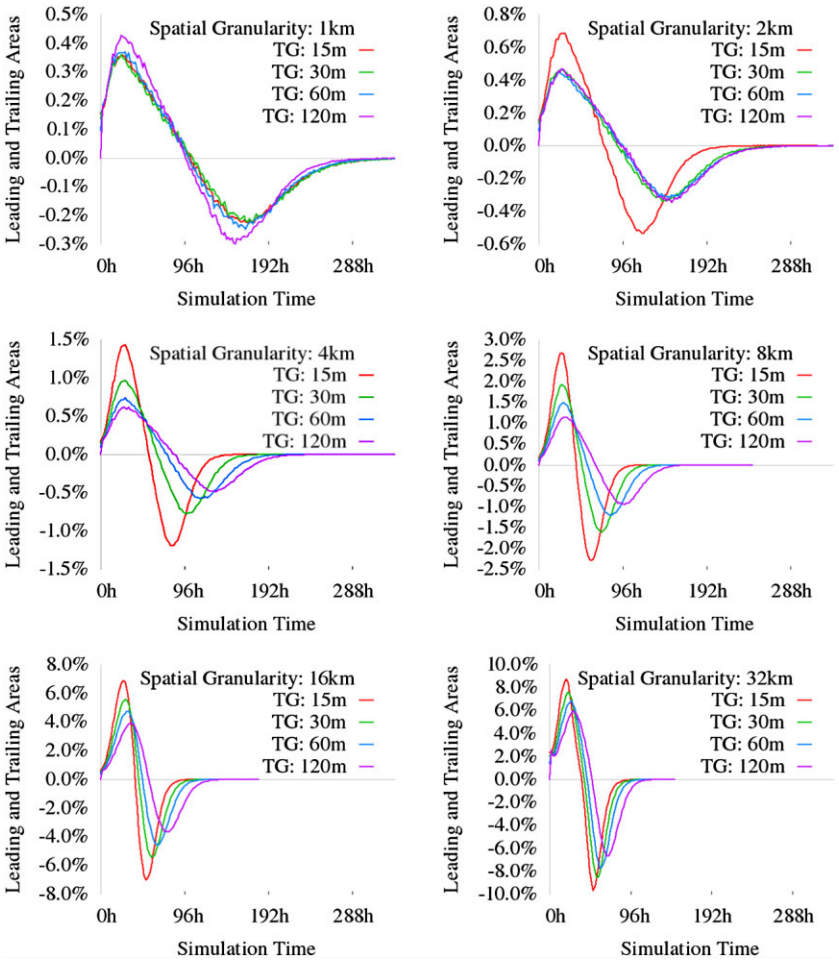

Figure 10. Swash-backwash model curves plotting increases in leading edge areas of disease spread as positive and increases in trailing edge areas of disease spread as negative for 8×8 km sized subareas.

that share a patch or nearby patch tends to increase (e.g., the average number of agents per patch ranges from $\frac{1}{16}$ to 64), which is evident when comparing a suite of maps at the TPAR for simulations that range from spatially fine grained to coarse grained (Fig. 11). Returning to the illustration of our infection model, agent C becomes infected in the SG = 4 cases (Fig. 5f). Yet, in the SG = 2 cases agent C cannot be infected (Fig. 5c), because the additional spatial information provided by finer spatial granularities establishes agent C as being too far away to be infected by agent E. In summary, the influence of coarsening spatial granularity on the two processes—movement and infection—results in faster spatial spread of disease as measured by higher peaks in leading edge areas, which in turn exposes more susceptible agents to disease and increases PAR and CAR.

We use a swash-backwash model to understand why coarsening temporal granularity generally increases the chance of disease burnout and slows down the speed of initial disease spread (Fig. 9a and 9b, respectively). The swash-backwash model results show that coarsening temporal

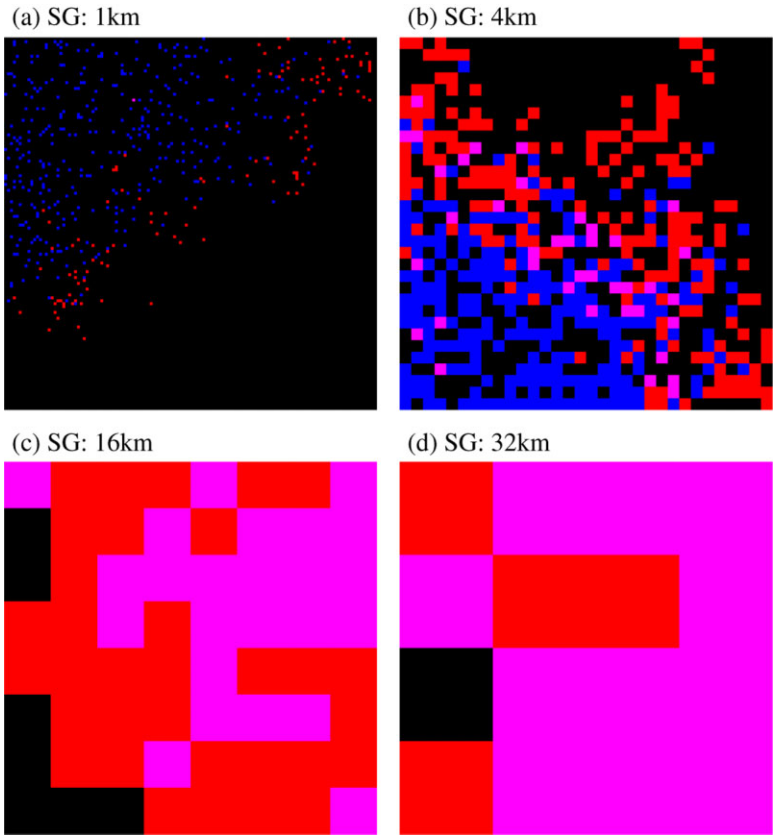

Figure 11. Maps at the time of peak attack rate for a suite of simulations with a temporal granularity of 15 m and spatial granularities (SG) ranging from 1 to 32 km. The average number of agents per patch ranges from $\frac{1}{16}$ to 64. Each patch in the map is drawn as a ratio of infected agents (red) to recovered agents (blue) on a black background.

granularity for a given spatial granularity generally leads to slower growth in leading edge areas (Fig. 10). Two factors contribute to this slower growth. First, temporally fine simulations enable agents to move further distances across a spatially coarsened landscape of patches. Because it is possible for an agent to move to an adjacent patch every time step, an agent may move across eight adjacent patches if temporal granularity is one compared with a single patch in the same time if temporal granularity is eight. The larger the patch size the greater distances an agent is potentially able to move in temporally fine-grained simulations compared with temporally coarse-grained simulations, which results in faster leading edge growth (Fig. 10). Second, coarsening temporal granularity introduces a temporal lag that affects subsequent infections as part of the infection process, which is analogous to compounding interest in a savings account. For example, a bank account with monthly compounding interest will earn less money over time compared with an account with daily compounding interest, because the earnings have fewer opportunities to compound on themselves each month compared with each day. Similarly, infectious agents have fewer opportunities to spread disease if temporal granularity is coarsened, and as a result, coarser temporal granularities in our experiments often exhibit slower initial

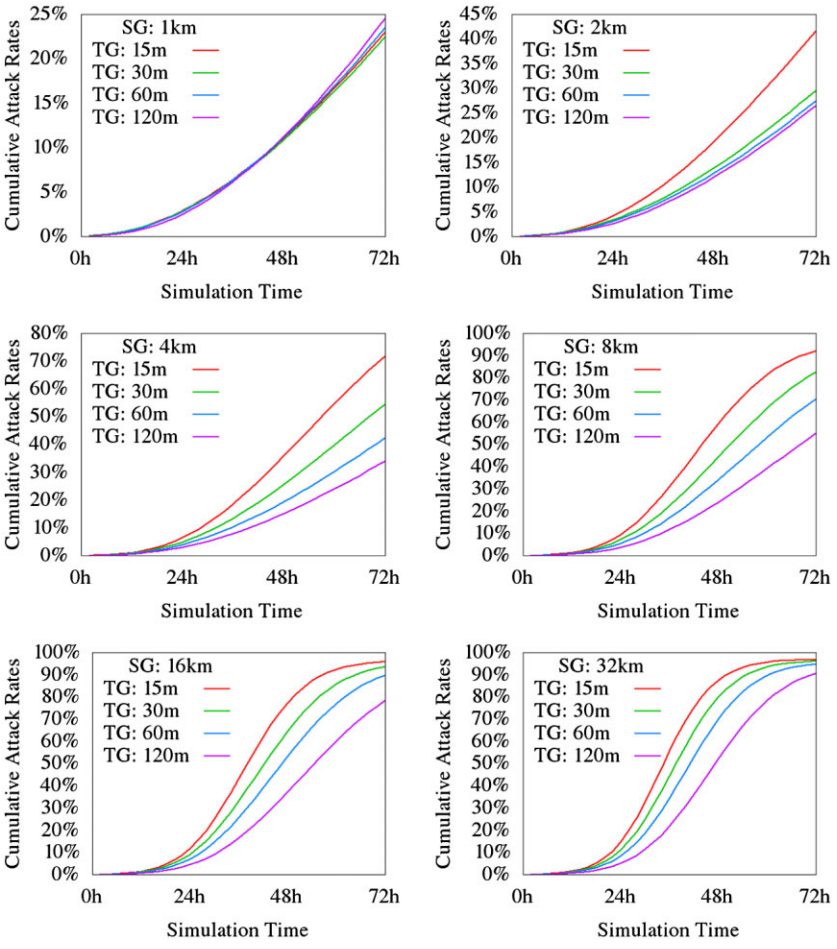

Figure 12. Cumulative attack rate curves plot accumulated infections as a percentage of total population. Simulation time for the first 72 h shown to illustrate initial disease spread.

disease spread as seen in cumulative attack curves that plot the accumulated number of infections across the duration of a simulation (Fig. 12). Generally, the influence of coarsening temporal granularity on the two processes leads to a decrease in the initial spatial spread as measured in leading edge area exposing fewer agents to disease, which slows the initial spread of disease (Fig. 9b) and in turn increases the chance of disease burnout (Fig. 9a). In summary, we find that coarsening STGs plays a significant role in influencing model processes that alter disease spread in epidemic ABMs.

Realistic community

To further examine the influence of STGs on disease spread dynamics in a more realistic context, we design a synthetic community ABM based on a widely used community-level population structure (Halloran et al. 2002; Longini et al. 2004; Germann et al. 2006). Our community ABM consists of 2,000 agents each associated with a household and either work, high school, middle school, elementary school, or daycare building. Agent and building populations are stochastically generated.

The ABM community is organized into four non-overlapping neighborhoods each containing roughly 500 agents. Households are assigned to a neighborhood and consist of at least one adult, and no more than seven individuals with approximately 33% being occupied by a single adult. Working adults (~70% of population) are randomly assigned to 1 of 70 work buildings of approximately 20 people. A community-wide high school (~155 students) and middle school (~128 students) service all neighborhoods. Two elementary schools (~79 students) each service two neighborhoods. Preschool children are assigned to one of two daycare centers in their neighborhood each having approximately 20 children.

To construct a spatially explicit community ABM, we use the following parameters not originally defined in Germann et al. (2006). The spatial extent of the community is 8×8 km to approximate the average population density of the United States. Each building is randomly located within a neighborhood and is sized based on the type of building (household, work, or school) and the number of occupants. We derive household sizes by multiplying the total number of persons in the household by 750 square feet based on the median square feet per person reported in an American Household Survey of the United States (Department of Housing and Urban Development 2011). We derive the size of a work building by multiplying the total number of workers in the building by 193 square feet based on findings in a Workspace Utilization and Allocation Benchmark that determined the private sector has a median 193 usable square feet per worker, which is comparable with a Federal benchmark of 190 usable square feet per worker (U.S. General Services Administration 2012). We derive the size of school and daycare buildings by multiplying the total number of students in the building by 154 square feet based on averaging the median square foot per student for elementary, middle, and high schools built in 2012 (School Planning and Management 2013).

Agents go to work, school, or daycare for 12 h and stay at home for 12 h as in Germann et al. (2006). This movement pattern is characteristic of daily commuting and is more realistic compared with the random walk process used in our parsimonious ABM. Each building may be situated on one or more patches depending on the size and location of a building and the spatial granularity (i.e., patch size). If a building is situated on more than one patch, then agents residing in the building will randomly select and move to one of the patches each time step. To provide an opportunity for random neighborhood contacts as described in Germann et al. (2006), our community ABM enables agents to leave their building and enter nearby buildings for 15-min time periods throughout the day and evening to meet colleagues, family, and friends, which is modeled as a random walk process from a starting patch on which the agent resides to nearby patches using the same infection model described in Agent Infection section. The combination of movement between home and work, school, or daycare (e.g., leaps through space) and nearby buildings provides hierarchical movement to our community ABM that was not present in our parsimonious ABM.

We use the following parameters for our community ABM experiments. Our community ABM simulates 2,000 agents for 30 days to explore early disease spread dynamics. Ten randomly selected agents are infected at the beginning of each simulation. Our community ABM uses a widely adopted epidemiological model of disease progression with four stages: susceptible, exposed, infectious, and recovered (Hethcote 2000). We set exposed and infectious periods of 4.1 and 1.2 days, respectively, as is used in Germann et al. (2006). Infectious agents attempt to infect susceptible agents within a radius of 2 m to approximate the distance of infection for influenza-like illness (Fiore et al. 2011) with 15% probability of infection. We examine three spatial granularities with edge lengths equal to 20, 40, and 80 m and three temporal granularities with

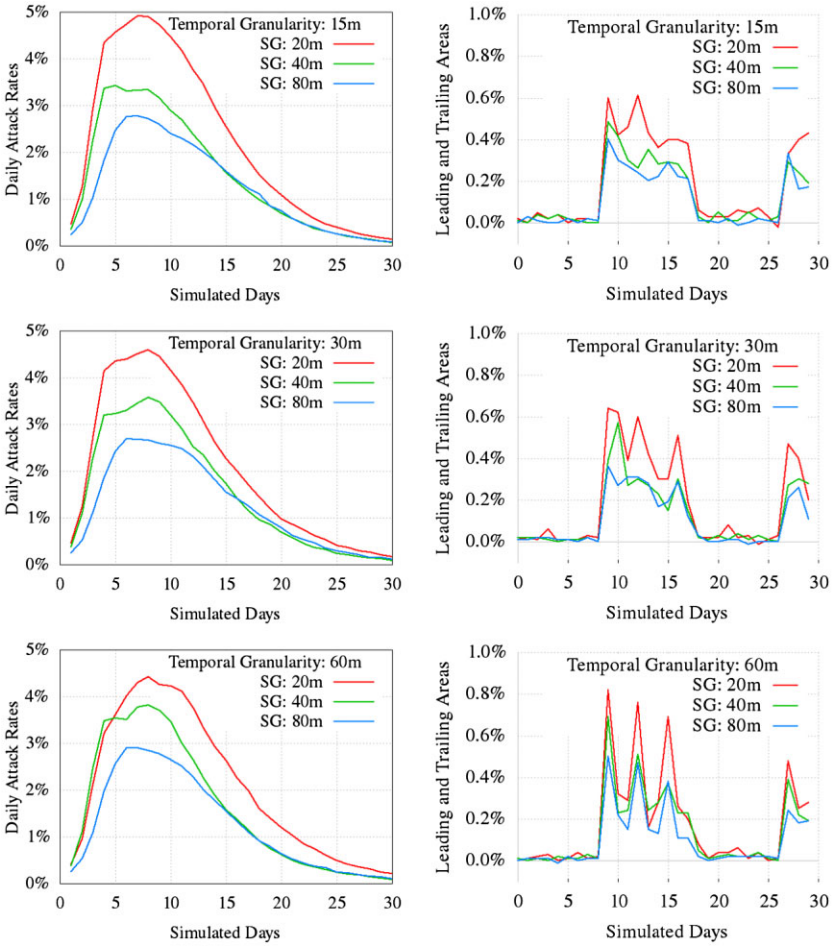

Figure 13. Plots experimental results for the community agent-based model including daily attack rates (left) and swash-backwash model results (right).

time step durations equal to 15, 30, and 60 min. The results are averaged over 100 simulations for each parameter configuration using 1,000,000 spatiotemporal process model executions.

Unlike the results of our parsimonious ABM, the attack rate curves for our community ABM show that coarsening spatial granularity generally reduces PAR and TPAR occurs earlier in a simulation (Fig. 13). We find that CARs for our community ABM also decline as spatial granularities are coarsened from an average of 63% (SG = 20 m) to 46% (SG = 40 m) and 37% (SG = 80 m). Differences in the influence of coarsening spatial granularities are partially attributed to hierarchical movement in our community ABM. Environmental constraints (e.g., agents residing within buildings) limit the distance an agent may travel when coarsening STGs compared with unconstrained random walks, which influence the spatial spread of disease (see previous discussion in Spatial Spread of Disease section). Unlike the results of our parsimonious ABM, the swash-backwash model results from our community ABM generally show little early spatial growth as disease spreads among family members and coworkers increasing the number of infected individuals, but not spatial area. At approximately day 8, there is considerable spatial growth for all simulations as disease begins to spread to new households, workplaces, and

schools, which is followed by an oscillation pattern of spatial growth that is attributed to differences between agents being at home and work or school including number of occupants, neighborhood associations, and building sizes. Interestingly, when comparing daily attack rate curves and swash-backwash model results, we find that disease spatially spreads very little in our community until approximately PAR, at which point it begins to spatially spread indicating a promising direction to explore spatially targeted intervention strategies. Coarsening temporal granularity results in a slight reduction in PAR for spatially fine-grained simulations and a slight increase in PAR for spatially coarse-grained simulations, and results in more extreme oscillation patterns in the swash-backwash model results (Fig. 13). Coarsening temporal granularity lengthens the time step duration providing infectious agents more time to infect nearby susceptibles in a single time step, which influences disease spread dynamics differently based on context including whether agents are at home with few family members to infect or school with many classmates leading to more extreme oscillation patterns.

Concluding discussion

We formulate spatiotemporal process models as a new approach to contextualize ABM processes within space and time and to enable our ABMs to adjust to different STGs. In the context of epidemic ABMs, our approach transforms a distance-based disease model to a patch-based one (Riley 2007), enabling the assumption of homogenously mixed populations (Hethcote 2000) to be relaxed by refining spatial granularities, similar to the way network-based epidemic models enable fully mixed populations to be relaxed by introducing network structure (Ferrari et al. 2011). This capability enables us to examine the results of simulations ranging from spatially and temporally coarse grained to fine grained, to understand the influence of not only spatial granularity, but also temporal granularity on model processes without the drawbacks of comparing models with differing assumptions (Kaplan and Wein 2003; Ajelli et al. 2010). Our study used simple processes as examples, but spatiotemporal process models can be designed for different spatial representations (e.g., polygons) or more complex processes such as spatial transmission kernels (Ajelli and Merler 2008) or improved pedestrian movement (Kerridge, Hine, and Wigan 2001).

Our study represents the first critical examination of how the representations of both space and time in a single epidemic ABM shape processes that operate within the constraints of such representations. The results of our study show that coarsening STGs influence model processes and subsequently disease spread in a parsimonious epidemic ABM. Specifically, we found that coarsening spatial granularity increases PAR by more than 6.5% and speeds TPAR by three times, which is consistent with related studies that observe increased attack rates with reduced spatial structure (Bobashev et al. 2007; Ajelli et al. 2010). Further, the chance of disease die-off (infecting less than 1% of a population) is reduced by more than two times. We also found that coarsening spatial granularity in our parsimonious ABM dramatically increases the speed of spatial spread of disease as measured by a swash-backwash model. On the other hand, we found that coarsening temporal granularity generally had the opposite effect resulting in decreased PAR, slowed down TPAR and initial spread of disease, and increased the chance of disease die-off.

We compare the results of our parsimonious and community ABMs and found differences in the influence of STGs. In our community ABM, coarsening spatial granularity decreases PAR by 2.2% and reduces the speed of spatial spread. Coarsening temporal granularity had less influence

on PAR and TPAR, but resulted in more extreme oscillation patterns in spatial growth as agents moved between home and work. The findings suggest that space–time representations may have complex interactions with spatial processes embedded in epidemic ABMs with certain representations potentially leading to increases in the number of infections in one context and decreases in another context. Epidemic ABMs designed for a single space–time representation are ill suited to realize these differences. In the future, ABMs may be designed to include space–time representations as variable parameters similar to walking speed or infection probability. In this way, modelers may use parameter fitting and sensitivity analysis to select the most appropriate space–time representation for their ABM.

Our study synergistically integrates both spatial and temporal perspectives to deepen understanding of the influence of STGs on epidemic ABM processes by spatially situating attack rate curves using the results of a swash-backwash model. This study is a first step in addressing a long-standing problem in epidemic modeling literature, namely how to systematically vary and study spatial structure (e.g., spatial granularities) in spatially explicit epidemic models while opening new opportunities to study temporal granularities, which until now have received little attention. As a first step, we sought parsimony in our ABM to gain systematic understanding of how changes in STGs impact disease spread similar to those works in network-based epidemic models (Keeling and Eames 2005; Xu and Sui 2009; Rahmandad and Sterman 2010). We extended our parsimonious ABM to a community ABM to examine the influence of STGs in a more realistic scenario to further improve our understanding, and plan to continue to build on this understanding in future studies. Our study found non-linear relationships between TPAR and PAR when varying STGs, whereas another study found linear relationships when altering network topologies (Xu and Sui 2009), and understanding these differences may improve understanding in contact network-based research (Salathé and Jones 2010; Cauchemez et al. 2011; Emch et al. 2012). Spatiotemporal process models may also be a first step toward designing new approaches and methodologies for ABMs to better handle spatial and temporal dependence.

Our future studies will also investigate the sensitivity of intervention strategies to STGs, elucidating any relationships between them, which Prieto et al. (2012) discusses with respect to simplifying assumptions and we briefly discussed in Realistic Community section. Generally, intervention strategies whether medical or mobility (McLafferty 2010) limit the potential distance of infection (e.g., travel restrictions) or the number of potential susceptibles (e.g., mass or targeted immunizations). Similarly, coarsening temporal granularity affects our movement process by reducing the number of patches infectious agents may move to, and refining spatial granularity affects our infection process by dividing larger spatial areas into many small areas limiting the number of potentially nearby susceptibles leading to a delay and decrease in PAR. It is therefore possible that simulations executed with certain STGs may over- or underestimate the effectiveness of an intervention due to their influence on model processes (e.g., discussed with respect to homogeneous mixing in Ferguson et al. 2003), which may help explain why three spatially structured ABMs respond differently to various intervention strategies (Halloran et al. 2008). An improved understanding of the influence of STGs on simulated intervention effectiveness could provide new insights for scholars and policy makers when faced with a future epidemic.

References

Ajelli, M., and S. Merler. (2008). "The Impact of the Unstructured Contacts Component in Influenza Pandemic Modeling." *PLoS ONE* 3(1), e1519.

Ajelli, M., B. Gonçalves, D. Balcan, V. Colizza, H. Hu, J. Ramasco, S. Merler, and A. Vespignani. (2010). "Comparing Large-Scale Computational Approaches to Epidemic Modeling: Agent-Based versus Structured Metapopulation Models." *BMC Infectious Diseases* 10(1), 190.

Albrecht, J. (2005). "A New Age for Geosimulation." *Transactions in GIS* 9(4), 451–4.

Anselin, L. (1995). "Local Indicators of Spatial Association—LISA." *Geographical Analysis* 27(2), 93–115.

Anselin, L., and S. Rey. (1991). "Properties of Tests for Spatial Dependence in Linear Regression Models." *Geographical Analysis* 23(2), 112–31.

Atti, M., S. Merler, C. Rizzo, M. Ajelli, M. Massari, P. Manfredi, C. Furlanello, G. Tomba, and M. Iannelli. (2008). "Mitigation Measures for Pandemic Influenza in Italy: An Individual Based Model Considering Different Scenarios." *PLoS ONE* 3(3), e1790.

Balcan, D., and A. Vespignani. (2012). "Invasion Threshold in Structured Populations with Recurrent Mobility Patterns." *Journal of Theoretical Biology* 293(0), 87–100.

Balcan, D., V. Colizza, B. Gonçalves, H. Hu, J. Ramasco, and A. Vespignani. (2009). "Multiscale Mobility Networks and the Spatial Spreading of Infectious Diseases." *Proceedings of the National Academy of Sciences of the United States of America* 106(51), 21484–9.

Balcan, D., B. Gonccalves, H. Hu, J. Ramasco, V. Colizza, and A. Vespignani. (2010). "Modeling the Spatial Spread of Infectious Diseases: The Global Epidemic and Mobility Computational Model." *Journal of Computational Science* 1(3), 132–45.

Batty, M. (2003). "Agent-Based Pedestrian Modelling." In *Advanced Spatial Analysis: The CASA Book of GIS*, 81–106, edited by P. Longley and M. Batty. Redlands, CA, USA: ESRI Press.

Batty, M. (2010). "Space, Scale, and Scaling in Entropy Maximizing." *Geographical Analysis* 42(4), 395–421.

Batty, M. (2012). "A Generic Framework for Computational Spatial Modelling." In *Agent-Based Models of Geographical Systems*, 19–50, edited by A. Heppenstall, A. Crooks, L. See and M. Batty. Dordrecht: Springer Netherlands.

Batty, M., A. Crooks, L. See, and A. Heppenstall. (2012). "Perspectives on Agent-Based Models and Geographical Systems." In *Agent-Based Models of Geographical Systems*, 1–15, edited by A. Heppenstall, A. Crooks, L. See and M. Batty. Dordrecht: Springer Netherlands.

Beyer, K., C. Tiwari, and G. Rushton. (2012). "Five Essential Properties of Disease Maps." *Annals of the Association of American Geographers* 102(5), 1067–75.

Bian, L. (2004). "A Conceptual Framework for an Individual-Based Spatially Explicit Epidemiological Model." *Environment and Planning B* 31(3), 381–96.

Bian, L. (2013). "Spatial Approaches to Modeling Dispersion of Communicable Diseases: A Review." *Transactions in GIS* 17(1), 1–17.

Bobashev, G., D. Goedecke, F. Yu, and J. Epstein. (2007). "A Hybrid Epidemic Model: Combining the Advantages of Agent-Based and Equation-Based Approaches." In *Proceedings of the 39th Conference on Winter Simulation (WSC)*, 1532–7. Piscataway, NJ, USA: IEEE Press.

Brockmann, D. (2009). "Human Mobility and Spatial Disease Dynamics." In *Reviews of Nonlinear Dynamics and Complexity*, 1–24, edited by H. Schuster. Heinheim: Wiley-VCH.

Brockmann, D., L. Hufnagel, and T. Geisel. (2006). "The Scaling Laws of Human Travel." *Nature* 439(7075), 462–5.

Cauchemez, S., A. Bhattarai, T. Marchbanks, R. Fagan, S. Ostroff, N. Ferguson *et al*. (2011). "Role of Social Networks in Shaping Disease Transmission during a Community Outbreak of 2009 H1N1 Pandemic Influenza." *Proceedings of the National Academy of Sciences of the United States of America* 108(7), 2825–30.

Chao, D., M. Halloran, V. Obenchain, and I. Longini. (2010). "FluTE, A Publicly Available Stochastic Influenza Epidemic Simulation Model." *PLoS Computational Biology* 6(1), e1000656.

Cliff, A., and P. Haggett. (2006). "A Swash-Backwash Model of the Single Epidemic Wave." *Journal of Geographical Systems* 8(3), 227–52.

Cliff, A., P. Haggett, and M. Smallman-Raynor. (2008). "An Exploratory Method for Estimating the Changing Speed of Epidemic Waves from Historical Data." *International Journal of Epidemiology* 37(1), 106–12.

Crooks, A., and C. Castle. (2012). "The Integration of Agent-Based Modelling and Geographical Information for Geospatial Simulation." In *Agent-Based Models of Geographical Systems*, 219–51, edited by A. Heppenstall, A. Crooks, L. See and M. Batty. Dordrecht: Springer Netherlands.

Danon, L., T. House, and M. Keeling. (2009). "The Role of Routine versus Random Movements on the Spread of Disease in Great Britain." *Epidemics* 1(4), 250–8.

Department of Housing and Urban Development. (2011). 2011 American Housing Survey for the United States. http://www.census.gov/housing/ahs/files/ahs11/National2011.xls (accessed June 1, 2014).

Emch, M., E. Root, S. Giebultowicz, M. Ali, C. Perez-Heydrich, and M. Yunus. (2012). "Integration of Spatial and Social Network Analysis in Disease Transmission Studies." *Annals of the Association of American Geographers* 102(5), 1004–15.

Epstein, J. (2009). "Modelling to Contain Pandemics." *Nature* 460(7256), 687–687.

Epstein, J., J. Parker, D. Cummings, and R. Hammond. (2008). "Coupled Contagion Dynamics of Fear and Disease: Mathematical and Computational Explorations." *PLoS ONE* 3(12), e3955.

Ferguson, N., M. Keeling, W. Edmunds, R. Gani, B. Grenfell, R. Anderson, and S. Leach. (2003). "Planning for Smallpox Outbreaks." *Nature* 425(6959), 681–5.

Ferguson, N., D. Cummings, C. Fraser, J. Cajka, P. Cooley, and D. Burke. (2006). "Strategies for Mitigating an Influenza Pandemic." *Nature* 442(7101), 448–52.

Ferrari, M., S. Perkins, L. Pomeroy, and O. Bjørnstad. (2011). "Pathogens, Social Networks, and the Paradox of Transmission Scaling." *Interdisciplinary Perspectives on Infectious Diseases* 2011(267049), 1–10.

Fiore, A., A. Fry, D. Shay, L. Gubareva, J. Bresee, and T. Uyeki. (2011). *Antiviral Agents for the Treatment and Chemoprophylaxis of Influenza*. Atlanta: Centers for Disease Control and Prevention.

Germann, T., K. Kadau, I. Longini, and C. Macken. (2006). "Mitigation Strategies for Pandemic Influenza in the United States." *Proceedings of the National Academy of Sciences of the United States of America* 103(15), 5935–40.

Goodchild, M. (2004). "Giscience, Geography, Form, and Process." *Annals of the Association of American Geographers* 94(4), 709–14.

Goodchild, M., and A. Glennon. (2008). "Representation and Computation of Geographic Dynamics." In *Understanding Dynamics of Geographic Domains*, 13–30, edited by K. Hornsby and M. Yuan. Boca Raton: CRC Press.

Grassly, N., and C. Fraser. (2008). "Mathematical Models of Infectious Disease Transmission." *Nature Reviews Microbiology* 6(6), 477–87.

Griffith, D. (2006). "Assessing Spatial Dependence in Count Data: Winsorized and Spatial Filter Specification Alternatives to the Auto-Poisson Model." *Geographical Analysis* 38(2), 160–79.

Grimm, V., U. Berger, F. Bastiansen, S. Eliassen, V. Ginot, J. Giske *et al*. (2006). "A Standard Protocol for Describing Individual-Based and Agent-Based Models." *Ecological Modelling* 198(1–2), 115–26.

Gumprecht, D., W. G. Müller, and J. Rodríguez-Díaz. (2009). "Designs for Detecting Spatial Dependence." *Geographical Analysis* 41(2), 127–43.

Hagen-Zanker, A., and Y. Jin. (2012). "A New Method of Adaptive Zoning for Spatial Interaction Models." *Geographical Analysis* 44(4), 281–301.

Haining, R., R. Kerry, and M. Oliver. (2010). "Geography, Spatial Data Analysis, and Geostatistics: An Overview." *Geographical Analysis* 42(1), 7–31.

Halloran, M., I. Longini, A. Nizam, and Y. Yang. (2002). "Containing Bioterrorist Smallpox." *Science* 298(5597), 1428–32.

Halloran, M., N. Ferguson, S. Eubank, I. Longini, D. Cummings, B. Lewis *et al*. (2008). "Modeling Targeted Layered Containment of an Influenza Pandemic in the United States." *Proceedings of the National Academy of Sciences of the United States of America* 105(12), 4639–44.

Hethcote, H. (2000). "The Mathematics of Infectious Diseases." *SIAM Review* 42(4), 599–653.

Hornsby, K., and M. J. Egenhofer. (2002). "Modeling Moving Objects over Multiple Granularities." *Annals of Mathematics and Artificial Intelligence* 36(1–2), 177–94.

Jiang, B., J. Yin, and S. Zhao. (2009). "Characterizing the Human Mobility Pattern in a Large Street Network." *Physical Review E* 80(2), 021136–21147.

Kaplan, E., and L. Wein. (2003). "Smallpox Bioterror Response." *Science* 300(5625), 1503–4.
Kareiva, P., A. Mullen, and R. Southwood. (1990). "Population Dynamics in Spatially Complex Environments: Theory and Data [and Discussion]." *Philosophical Transactions of the Royal Society of London. Series B: Biological Sciences* 330(1257), 175–90.
Keeling, M. (1999). "The Effects of Local Spatial Structure on Epidemiological Invasions." *Proceedings of the Royal Society of London. Series B: Biological Sciences* 266(1421), 859–67.
Keeling, M., and K. Eames. (2005). "Networks and Epidemic Models." *Journal of the Royal Society Interface* 2(4), 295–307.
Keeling, M., L. Danon, M. Vernon, and T. House. (2010). "Individual Identity and Movement Networks for Disease Metapopulations." *Proceedings of the National Academy of Sciences of the United States of America* 107(19), 8866–70.
Kerridge, J., J. Hine, and M. Wigan. (2001). "Agent-Based Modelling of Pedestrian Movements: The Questions that Need to be Asked and Answered." *Environment and Planning B* 28(3), 327–42.
Koopman, J. (2004). "Modeling Infection Transmission." *Annual Review of Public Health* 25, 303–26.
Kulldorff, M., and N. Nagarwalla. (1995). "Spatial Disease Clusters: Detection and Inference." *Statistics in Medicine* 14(8), 799–810.
Laskowski, M., B. Demianyk, J. Witt, S. Mukhi, M. Friesen, and R. McLeod. (2011). "Agent-Based Modeling of the Spread of Influenza-like Illness in an Emergency Department: A Simulation Study." *IEEE Transactions on Information Technology in Biomedicine: A Publication of the IEEE Engineering in Medicine and Biology Society* 15(6), 877–89.
Liu, X., and C. Andersson. (2004). "Assessing the Impact of Temporal Dynamics on Land-Use Change Modeling." *Computers, Environment and Urban Systems* 28(1–2), 107–24.
Longini, I., M. Halloran, A. Nizam, and Y. Yang. (2004). "Containing Pandemic Influenza with Antiviral Agents." *American Journal of Epidemiology* 159(7), 623–33.
Maantay, J., and S. McLafferty. (2011). "Environmental Health and Geospatial Analysis: An Overview." In *Geospatial Analysis of Environmental Health*, 3–37, edited by J. Manaatay and S. McLaffery. New York: Springer.
Manson, S., S. Sun, and D. Bonsal. (2012). "Agent-Based Modeling and Complexity." In *Agent-Based Models of Geographical Systems*, 125–39, edited by A. Heppenstall, A. Crooks, L. See and M. Batty. Dordrecht: Springer Netherlands.
McLafferty, S. (2010). "Placing Pandemics: Geographical Dimensions of Vulnerability and Spread." *Eurasian Geography and Economics* 51(2), 143–61.
Mishra, S., D. Fisman, and M. Boily. (2011). "The ABC of Terms Used in Mathematical Models of Infectious Diseases." *Journal of Epidemiology and Community Health* 65(1), 87–94.
O'Sullivan, D., J. Millington, G. Perry, and J. Wainwright. (2012). "Agent-Based Models—Because They're Worth It? *Agent-Based Models of Geographical Systems*, 85–105, edited by A. Heppenstall, A. Crooks, L. See and M. Batty. Dordrecht: Springer Netherlands.
Openshaw, S. (1983). *The Modifiable Areal Unit Problem*. Norwich: Geo Books Norwich.
Parker, D., S. Manson, M. Janssen, M. Hoffmann, and P. Deadman. (2003). "Multi-Agent Systems for the Simulation of Land-Use and Land-Cover Change: A Review." *Annals of the Association of American Geographers* 93(2), 314–37.
Parker, J., and J. Epstein. (2011). "A Distributed Platform for Global-Scale Agent-Based Models of Disease Transmission." *ACM Transactions on Modeling and Computer Simulation (TOMACS)* 22(1), 2.
Pearson, K. (1905). "The Problem of the Random Walk." *Nature* 72(1865), 294.
Perumalla, K., and S. Seal. (2011). "Discrete Event Modeling and Massively Parallel Execution of Epidemic Outbreak Phenomena." *Simulation* 88(7), 768–83.
Peuquet, D. (1994). "It's about Time: A Conceptual Framework for the Representation of Temporal Dynamics in Geographic Information Systems." *Annals of the Association of American Geographers* 84, 441–61.
Prieto, D., T. Das, A. Savachkin, A. Uribe, R. Izurieta, and S. Malavade. (2012). "A Systematic Review to Identify Areas of Enhancements of Pandemic Simulation Models for Operational Use at Provincial and Local Levels." *BMC Public Health* 12(1), 251.

Rahmandad, H., and J. Sterman. (2010). "Heterogeneity and Network Structure in the Dynamics of Diffusion: Comparing Agent-Based and Differential Equation Models." *Management Science* 54(5), 998–1014.

Reitsma, F., and J. Albrecht. (2005). "Implementing a New Data Model for Simulating Processes." *International Journal of Geographical Information Science* 19(10), 1073–90.

Riley, S. (2007). "Large-Scale Spatial-Transmission Models of Infectious Disease." *Science* 316(5829), 1298–301.

Roche, B., J. Drake, and P. Rohani. (2011). "An Agent-Based Model to Study the Epidemiological and Evolutionary Dynamics of Influenza Viruses." *BMC Bioinformatics* 12(1), 87.

Salathé, M., and J. Jones. (2010). "Dynamics and Control of Diseases in Networks with Community Structure." *PLoS Computational Biology* 6(4), e1000736.

Sattenspiel, L., and K. Dietz. (1995). "A Structured Epidemic Model Incorporating Geographic Mobility among Regions." *Mathematical Biosciences* 128(1–2), 71–91.

School Planning and Management. (2013). 2013 Annual School Construction Report. http://webspm.com/research/2013/02/annual-school-construction-report/asset.aspx (accessed June 1, 2014).

Shirley, M., and S. Rushton. (2005). "The Impacts of Network Topology on Disease Spread." *Ecological Complexity* 2(3), 287–99.

Smieszek, T. (2009). "A Mechanistic Model of Infection: Why Duration and Intensity of Contacts Should Be Included in Models of Disease Spread." *Theoretical Biology and Medical Modelling* 6(1), 25.

Smieszek, T., M. Balmer, J. Hattendorf, K. Axhausen, J. Zinsstag, and R. Scholz. (2011). "Reconstructing the 2003/2004 H3N2 Influenza Epidemic in Switzerland with a Spatially Explicit, Individual-Based Model." *BMC Infectious Diseases* 11(1), 115.

Snow, J. (1855). *On the Mode of Communication of Cholera*, 2nd ed. London: John Churchill.

Stanilov, K. (2012). "Space in Agent-Based Models." In *Agent-Based Models of Geographical Systems*, 253–69, edited by A. Heppenstall, A. Crooks, L. See and M. Batty. Dordrecht: Springer Netherlands.

U.S. General Services Administration. (2012). Workspace Utilization and Allocation Benchmark. http://www.gsa.gov/graphics/ogp/Workspace_Utilization_Banchmark_July_2012.pdf (accessed June 1, 2014).

Wainer, G., and P. Mosterman. (2011). *Discrete-Event Modeling and Simulation: Theory and Applications*. Boca Raton, FL, USA: CRC Press.

Wheaton, W., J. Cajka, B. Chasteen, D. Wagener, P. Cooley, L. Ganapathi, D. Roberts, and J. Allpress. (2009). Synthesized population databases: A US geospatial database for agent-based models. http://www.rti.org/pubs/mr-0010-0905-wheaton.pdf (Accessed: March, 2013).

Wong, D. (2009). "The Modifiable Areal Unit Problem (MAUP)." In *The Sage Handbook of Spatial Analysis*, 105–24, edited by A. Fotheringham and P. Rogerson. London: Sage Publications Limited.

Xu, Z., and D. Sui. (2009). "Effect of Small-World Networks on Epidemic Propagation and Intervention." *Geographical Analysis* 41(3), 263–82.

Yuan, M. (2001). "Representing Complex Geographic Phenomena in GIS." *Cartography and Geographic Information Science* 28(2), 83–96.

Zeigler, B., H. Praehofer, and T. Kim. (2000). *Theory of Modeling and Simulation: Integrating Discrete Event and Continuous Complex Dynamic Systems*. London: Academic Press.